

The Ratio, ρ , of the Real to the Imaginary Part of the
 $\bar{p}p$ Forward Elastic Scattering Amplitude at $\sqrt{s} = 1.8$ TeV

E-811 Collaboration

C. Avila^{a,b}, W. F. Baker^c, R. DeSalvo^{d*},
D. P. Eartly^c, C. Guss^{a**}, H. Jostlein^c,
M. R. Mondardini^{a***}, J. Orear^a, S. M. Pruss^c,
R. Rubinstein^c, S. Shukla^{c****}, F. Turkot^c

^a Cornell University, Ithaca, New York 14853, USA

^b Universidad de los Andes, Bogota, Colombia

^c Fermi National Accelerator Laboratory, Batavia, Illinois, 60510, USA

^d CERN, Geneva, Switzerland

Abstract

We have measured ρ , the ratio of the real to the imaginary part of the $\bar{p}p$ forward elastic scattering amplitude, at $\sqrt{s} = 1.8$ TeV. Our result is $\rho = 0.132 \pm 0.056$; this can be combined with a previous measurement at the same energy to give $\rho = 0.135 \pm 0.044$.

Measurements of ρ , the ratio of the real to the imaginary part of the forward $\bar{p}p$ elastic scattering amplitude, together with measurements of pp and $\bar{p}p$ total cross sections and some very general assumptions, allow prediction of total cross section behavior at considerably higher energies than are presently available^(1, 2). We report here a measurement of ρ at $\sqrt{s} = 1.8$ TeV, made at the same time as our Fermilab Tevatron measurement⁽³⁾ of the total cross section, σ_T . Previous measurements of ρ at $\bar{p}p$ colliders have been made at the ISR⁽⁴⁾, the SPS⁽⁵⁾, and the Tevatron⁽⁶⁾.

The experimental apparatus and method have been described in Reference 3; the major difference in the measurements reported here is analysis of data at smaller $|t|$ values, in order to study the $|t|$ region where Coulomb effects become important.

After event selection for elastic candidates as described in Reference 3, the data for a typical run are illustrated in Figure 1; a) shows the correlation for each event between the vertical (Y) coordinates of particles in proton and antiproton conjugate

detectors, while b) shows the corresponding horizontal (X) correlation. Elastic events are in the diagonal bands in each figure, with background increasing towards the region closest to the beams, as can be seen most clearly in Figure 1a). We would expect that the background is due to uncorrelated particles in the detectors caused by, for example, beam halo; which is known to increase sharply close to the beams. We used two methods to remove the remaining background under the elastic signal.

- A. Events in the elastic region were removed from the $X_{\text{proton}}-X_{\text{antiproton}}$ distribution; the $Y_{\text{proton}}-Y_{\text{antiproton}}$ correlation of the remaining events allowed determination of the background under the elastic region of the $Y_{\text{proton}}-Y_{\text{antiproton}}$ distribution.
- B. We used in the $Y_{\text{proton}}-Y_{\text{antiproton}}$ distribution only those events in the elastic region of the $X_{\text{proton}}-X_{\text{antiproton}}$ distribution. We then determined an analytic expression for the combined signal and background shapes perpendicular to the elastic correlation of Figure 1a) in the region with lower background. This analytic form was extrapolated into the small $Y_{\text{proton}}-Y_{\text{antiproton}}$ region to determine the background in that region.

Methods A and B for background subtraction gave identical results, within statistical uncertainties, for ρ ; results are quoted using method A. Our analysis used data in the range $0.002 < |t| < 0.035$ (GeV/c^2); at the smallest $|t|$, up to 70% of the events were background, but this dropped rapidly with increasing $|t|$; however, the background could be determined with sufficient statistical precision, and our final statistical uncertainties include the contribution from the background determination. The number of elastic events used in this analysis was about 40,000.

We use the following expression for the elastic differential cross section:

$$\begin{aligned}
 \frac{1}{L} \frac{dN_{el}}{dt} &= \frac{d\sigma}{dt} = \frac{4\pi\alpha^2 (\hbar c)^2 G^4(t)}{|t|^2} \\
 &+ \frac{\alpha(\rho - \alpha\phi)\sigma_T G^2(t)}{|t|} \exp(-B|t|/2) \\
 &+ \frac{\sigma_i^2 (1 + \rho^2)}{16\pi(\hbar c)^2} \exp(-B|t|).
 \end{aligned} \tag{1}$$

The three terms in Equation (1) are due to, respectively, Coulomb scattering, Coulomb-nuclear interference, and nuclear scattering. L is the integrated accelerator luminosity, dN_{el}/dt is the observed elastic differential distribution, α is the fine structure constant, ϕ is the relative Coulomb-nuclear phase, given by⁽⁷⁾ $\ln(0.08|t|^{-1}) - 0.577$, and $G(t)$ is the nucleon electromagnetic form factor, which we parameterize in the usual way as $(1+|t|/0.71)^{-2}$ [t is in $(\text{GeV}/c)^2$].

We also use the following two equations:

$$\sigma_T^2 = \frac{1}{L} \frac{16\pi(\hbar c)^2}{(1+\rho^2)} \left. \frac{dN_{el}^n}{dt} \right|_{t=0} \quad (2)$$

$$\sigma_T = \frac{1}{L} (N_{el}^n + N_{inel}) \quad (3)$$

Equation (2) is obtained from the optical theorem. N_{el}^n is the total number of nuclear elastic events, obtained from the observed dN_{el}/dt distribution in the t region where nuclear scattering dominates, and extrapolated to $t=0$ and $t=\infty$ using the form $\exp(-B|t|)$. $dN_{el}^n/dt|_{t=0}$ is the observed differential number of nuclear elastic events extrapolated to $t=0$ using the same form. N_{inel} is the total number of inelastic events; our method for obtaining this, using detectors close to the interaction point, has been described earlier⁽³⁾. Note that Equations (2) and (3) allow us to express L in terms of σ_T and ρ . Then dN_{el}/dt in Equation (1) can be expressed in terms of just two unknowns, σ_T and ρ . Our input data are our measurements of dN_{el}/dt together with the total number of inelastic events N_{inel} for the same runs as the elastic data, and the value of $B = 16.98 \pm 0.22$ $(\text{GeV}/c)^{-2}$ (the mean from Refs. 6 and 8). We carry out a least-squares analysis for σ_T and ρ in Equation (1) using all of our input data.

The result of the fit is

$$\sigma_T = 71.42 \pm 1.55 \text{ mb}; \quad \rho = 0.132 \pm 0.049$$

where the uncertainties quoted are statistical only. In this fit the χ^2 per degree of freedom is 1.05. We show in Figure 2 the fit to our dN_{el}/dt data, together with two

other fits for illustration, fixing $\rho = 0$ and 0.24 as noted, and allowing only σ_T to vary; these latter two fits both give χ^2 per degree of freedom of 1.4.

We considered 11 sources of systematic uncertainties, with the major ones including the uncertainties in N_{inel} and B , cuts on the elastic event sample, detector calibrations and efficiencies, and detector positions with respect to the beam center. Almost all of these were obtained from our own data, with uncertainties that were statistical. These systematic uncertainties total ± 1.85 mb in σ_T and ± 0.028 in ρ . Combining statistical and systematic uncertainties in quadrature leads to our final result of

$$\sigma_T = 71.42 \pm 2.41 \text{ mb}; \quad \rho = 0.132 \pm 0.056$$

The value of σ_T given here⁽⁹⁾ supercedes that of Ref. 3.

Our value of ρ is identical within uncertainties to that of E710⁽⁶⁾. We can combine the two results in quadrature (since there is little common systematic uncertainty) to give a value at $\sqrt{s} = 1.8$ TeV of

$$\rho = 0.135 \pm 0.044$$

This value is shown in Figure 3, together with results at lower energies^(4, 5, 10), and a prediction⁽¹¹⁾ based on existing ρ and pp and $\bar{p}p$ σ_T data. Using the approximate asymptotic dispersion relation⁽²⁾.

$$\rho \approx \frac{\pi}{2\sigma_T} \frac{d\sigma_T}{d(\log s)}$$

we find consistency between our values of ρ and σ_T and previous lower energy σ_T data.

In summary, we have made a new measurement of ρ at $\sqrt{s} = 1.8$ TeV, which confirms previous data with higher accuracy, and provides a consistent picture, via an approximate dispersion relation, with our measurement and lower energy σ_T data.

Acknowledgements

This work was supported by the US Department of Energy and the US National Science Foundation. We are grateful for support and initial detector development by

the Small Angle Subgroup of the CERN LAA Lab, especially C. Davis, M. Lundin and A. Zichichi. We received invaluable aid from the Fermilab Accelerator, Computing, and Research Divisions, and the Physics Section. We thank A. Baumbaugh and K. Knickerbocker for the design, construction, and testing of the fiber detector readout system, and also N. Amos, C. McClure, and N. Gelfand for their interest and assistance.

References

- * Present address: California Institute of Technology, Pasadena, California, 91125, USA
 - ** Present address: 1212 Pine Ave., Montreal PQ, H3G 1A9, Canada
 - *** Present address: ETT Division, CERN, CH-1211 Geneva 23, Switzerland
 - **** Present address: CMS Energy, Houston, Texas, USA
1. C. Augier et al., Phys. Lett. B315, 503, 1993; M. M. Block et al., Phys. Rev. D45, 839 (1999), and earlier references cited therein.
 2. M. M. Block, K. Kang, A. R. White, Int. Journ. Mod. Phys. A7, 4449 (1992).
 3. C. Avila et al., Phys. Lett. B 445, 419 (1999).
 4. N. A. Amos et al., Nucl. Phys. B 262, 689 (1985).
 5. C. Augier et al., Phys. Lett. B 316, 448 (1993).
 6. N. A. Amos et al., Phys. Rev. Lett. 68, 2433 (1992).
 7. G. B. West and D. R. Yennie, Phys. Rev. 172, 1413 (1968).
 8. F. Abe et al., Phys. Rev. D50, 5518 (1994).
 9. Note that this value of σ_T has a larger uncertainty than that of Ref 3. In some previous measurements (e.g. Ref 3 and F. Abe et al., Phys. Rev. D 50, 5550, 1994) the quantity actually measured is $\sigma_T(1+\rho^2)$, and a value of ρ is assumed from dispersion relation fits, with the uncertainty in ρ set to zero. In the current measurement, we do a two-parameter fit to σ_T and ρ , and the uncertainty in ρ affects the final uncertainty in σ_T .
 10. L. Fajardo et al., Phys. Rev. D 24, 46 (1981).
 11. The curve shown is from dispersion relations, and is similar to and consistent with that of C. Augier et al. (Ref. 1). An essentially identical curve is also obtained by M. M. Block et al (Ref. 1).

Figure Captions

Figure 1

- a) Correlation between the vertical (Y) coordinates of events in the proton and antiproton conjugate detectors.
- b) Correlation between the horizontal (X) coordinates of events in the proton and antiproton conjugate detectors.

The center of the Tevatron proton and antiproton beams is at X=Y=0.

Figure 2.

Our $\frac{dN_{el}}{dt}$ data with (solid line) our best fit ($\rho = 0.132$), as described in the text. The dashed curve is the best fit fixing $\rho = 0$, and the dot-dashed curve is the best fit fixing $\rho = 0.24$.

Figure 3.

The result for ρ of this experiment (E-811) combined with that of Ref. 6 (E-710), together with results from lower energies (Refs. 4, 5, 10) and a curve (Ref. 11) showing the prediction based on existing pp , $\bar{p}p$ and ρ data.

Disclaimer

Operated by Universities Research Association Inc. under
Contract No. DE-AC02-76CH03000 with the United States Department of Energy.

This report was prepared as an account of work sponsored by an agency of the United States Government. Neither the United States Government nor any agency thereof, nor any of their employees, makes any warranty, express or implied, or assumes any legal liability or responsibility for the accuracy, completeness, or usefulness of any information, apparatus, product, or process disclosed, or represents that its use would not infringe privately owned rights. Reference herein to any specific commercial product, process, or service by trade name, trademark, manufacturer, or otherwise, does not necessarily constitute or imply its endorsement, recommendation, or favoring by the United States Government or any agency thereof. The views and opinions of authors expressed herein do not necessarily state or reflect those of the United States Government or any agency thereof.

Approved for public release; further dissemination unlimited.

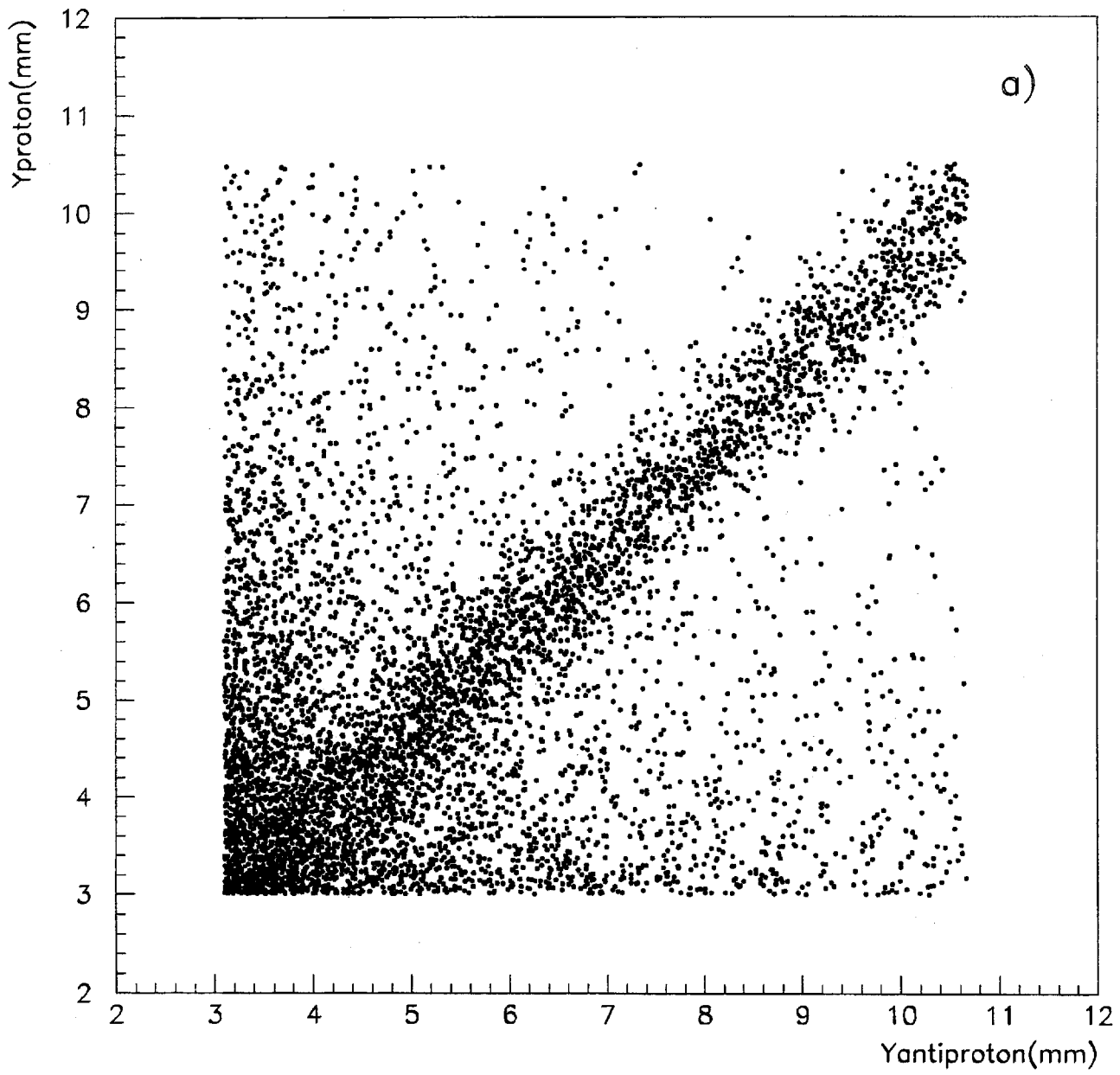


Figure 1 a)

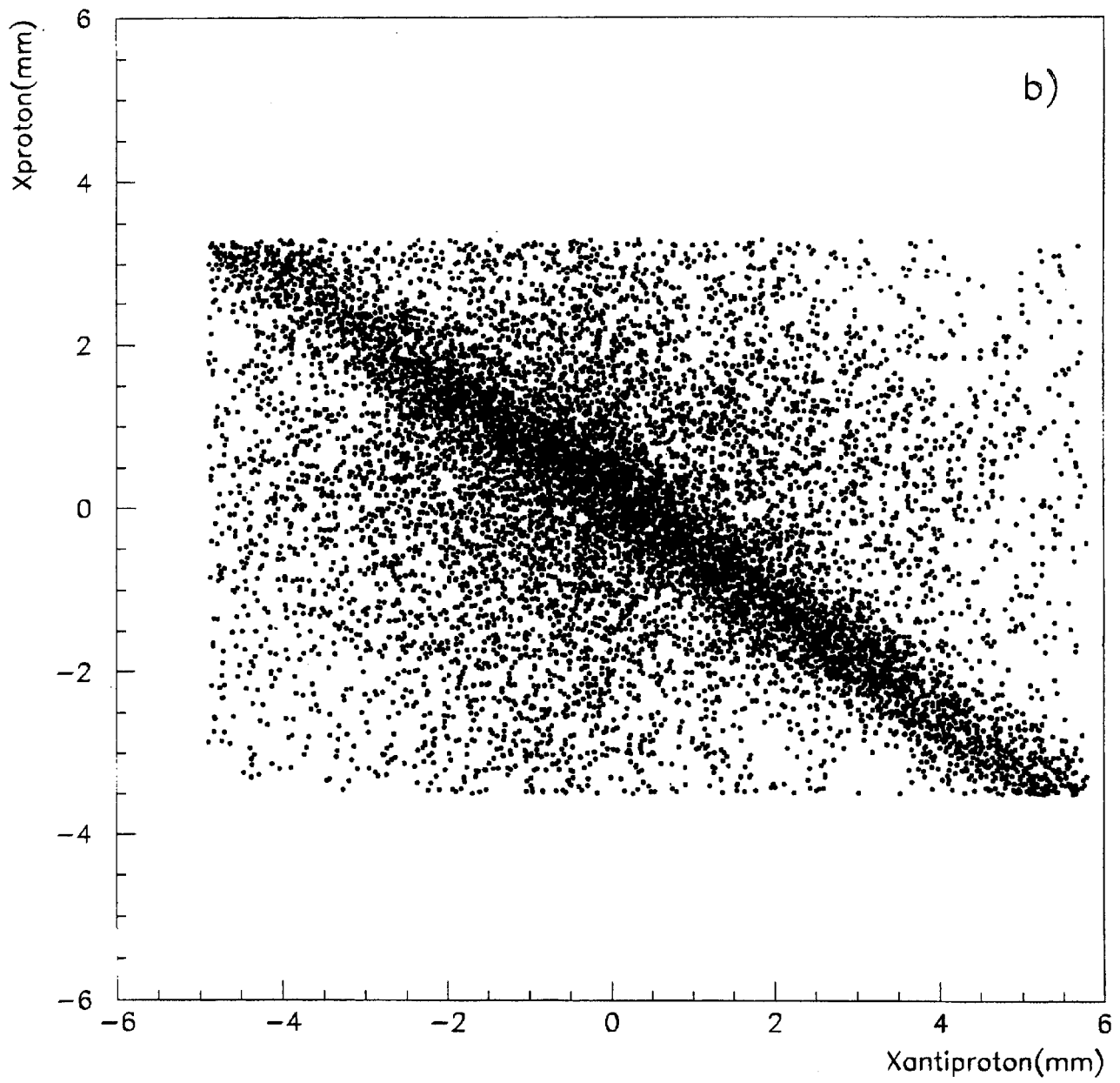


Figure 1 b)

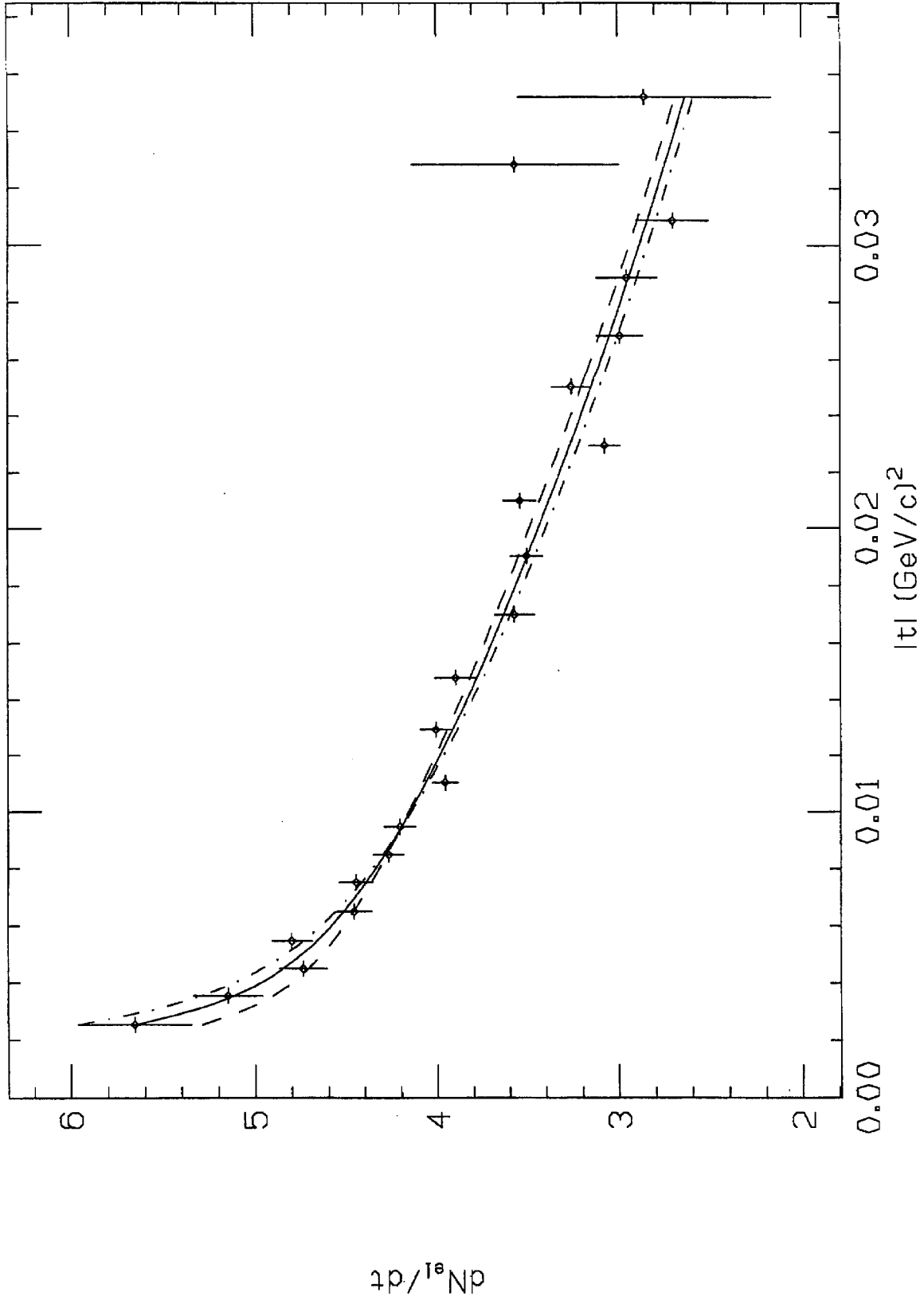


Figure 2

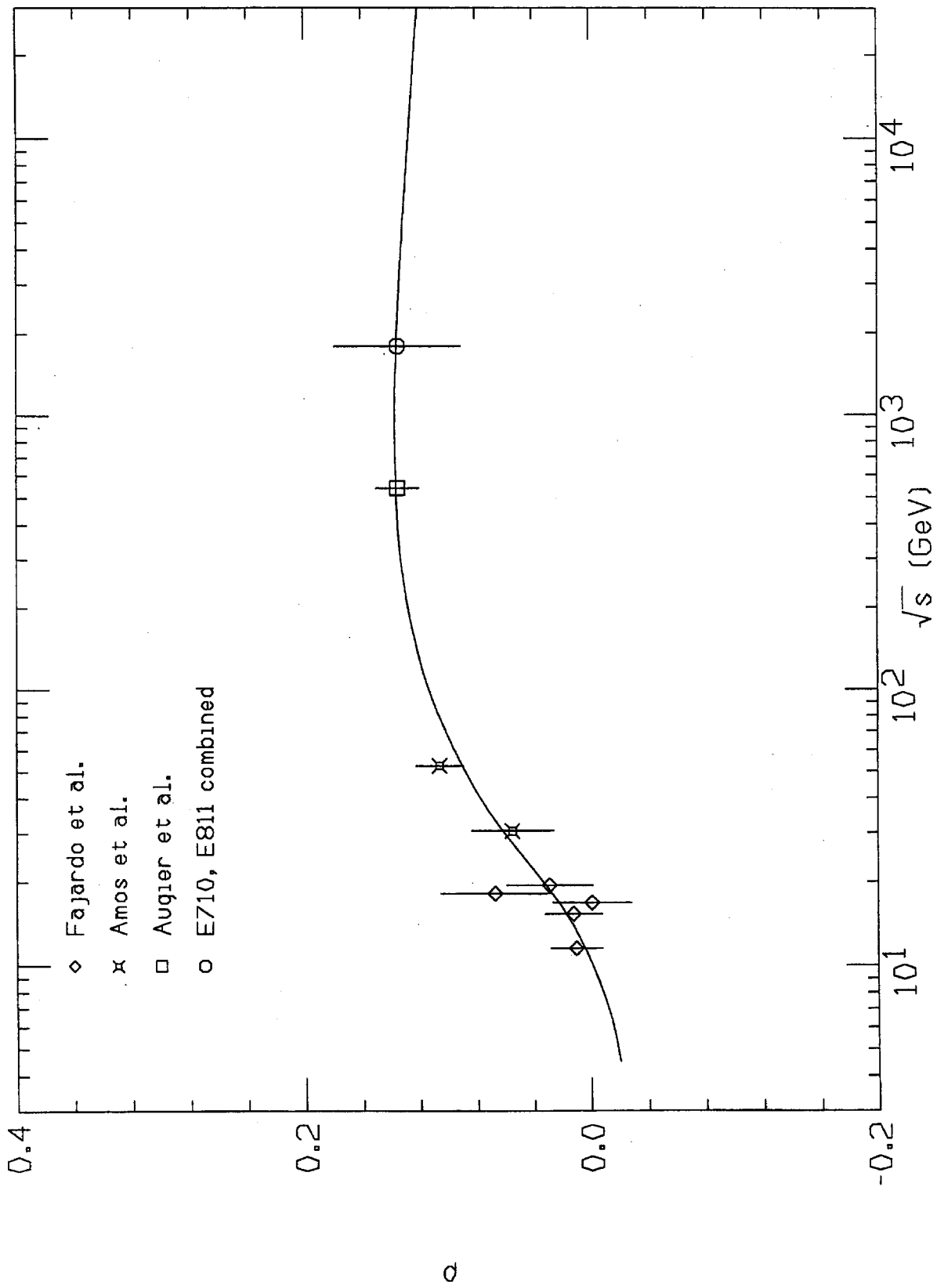


Figure 3